

# Lab on a Chip

Accepted Manuscript



This article can be cited before page numbers have been issued, to do this please use: M. Yang, R. Liu, M. Ripoll and K. Chen, *Lab Chip*, 2015, DOI: 10.1039/C5LC00479A.



This is an *Accepted Manuscript*, which has been through the Royal Society of Chemistry peer review process and has been accepted for publication.

*Accepted Manuscripts* are published online shortly after acceptance, before technical editing, formatting and proof reading. Using this free service, authors can make their results available to the community, in citable form, before we publish the edited article. We will replace this *Accepted Manuscript* with the edited and formatted *Advance Article* as soon as it is available.

You can find more information about *Accepted Manuscripts* in the [Information for Authors](#).

Please note that technical editing may introduce minor changes to the text and/or graphics, which may alter content. The journal's standard [Terms & Conditions](#) and the [Ethical guidelines](#) still apply. In no event shall the Royal Society of Chemistry be held responsible for any errors or omissions in this *Accepted Manuscript* or any consequences arising from the use of any information it contains.

# A microscale turbine driven by diffusive mass flux

Mingcheng Yang,<sup>1,\*</sup> Rui Liu,<sup>1</sup> Marisol Ripoll,<sup>2</sup> and Ke Chen<sup>1,†</sup>

View Article Online  
DOI: 10.1039/C5LC00479A

<sup>1</sup>Beijing National Laboratory for Condensed Matter Physics and Key Laboratory of Soft Matter Physics, Institute of Physics, Chinese Academy of Sciences, Beijing 100190, China

<sup>2</sup>Theoretical Soft-Matter and Biophysics, Institute of Complex Systems, Forschungszentrum Jülich, 52425 Jülich, Germany

An external diffusive mass flux is shown to be able to generate a mechanical torque on a microscale object based on anisotropic diffusiophoresis. In light of this finding, we propose a theoretical prototype micro-turbine driven purely by diffusive mass flux, which is in strong contrast to conventional turbines driven by convective mass flows. The rotational velocity of the proposed turbine is determined by the external concentration gradient, the geometry and the diffusiophoretic properties of the turbine. This scenario is validated by performing computer simulations. Our finding thus provides a new type of chemo-mechanical response which could be used to exploit existing chemical energies at small scales.

PACS numbers: 66.10.C-, 07.10.Cm, 02.70.Ns

## INTRODUCTION

As a fundamental microscopic process, diffusion is at the heart of many physical, chemical and biological phenomena [1]. Besides mass transportation, diffusive fluxes induced by concentration gradients also carry exploitable chemical energy. Concentration inhomogeneities are ubiquitous in nature, from the estuary of rivers to the inside of living cells. In particular, chemical gradients are becoming an essential ingredient for lab-on-chip research, which can be generated by different microfluidic gradient-generators [2–6]. Harnessing the chemical energy in existing concentration gradients is therefore of great practical and fundamental importance. So far, all the strategies proposed are based on (partially) ion-selective transport through electrodes, membranes or nano-pores [7–11], and most of them convert chemical energy into electrical energy. On nano- and microscales, it would be more convenient and versatile to utilize this energy if direct conversion to mechanical energy could be achieved.

It is known that diffusive and convective mass flows can exert mechanical forces on an immersed object by diffusiophoretic effect [12–14] and deflection of the momenta of macroscopic particle flow, respectively. Inspired by this apparent resemblance and the fact that convective flows can produce a torque to drive a turbine, one interesting question is whether an external curl-free diffusive mass flux can generate a torque on a microscale turbine-like structure. If the answer is positive, such chemo-mechanical effect will be particularly suitable for designing miniaturized machines, and would find many potential applications.

In this work, we propose a scheme to obtain a torque from an external diffusive mass flux. The principle is based on anisotropic diffusiophoresis, by which an external concentration gradient can lead to a perpendicular mechanical driving force on a non-spherical immersed object. With this scheme we construct theoretically a

microscale turbine that can unidirectionally rotate in an external concentration gradient. Its validity is verified by performing state-of-the-art computer simulations. This diffusiophoretic microturbine is driven by purely diffusive particle flux, which is conceptually different from conventional turbines driven by convective particle fluxes. Therefore, the proposed chemo-mechanical scheme allows one to harvest mechanical work directly from the external concentration gradient. This opens up promising new routes to design chemical gradient-driven devices such as micro-motors, pumps, mixers, or sensors to control local microfluidic chemical gradients.

## THEORY: ANISOTROPIC DIFFUSIOPHORESIS AND DIFFUSIOPHORETIC MICROTURBINE

In solutions with spatial variation of solute concentration, suspended particles can suffer from mechanical driving force and hence drift along the gradient. This phenomenon is known as diffusiophoresis [12–16], and belongs to the general class of phoretic effects including eletro- and thermophoresis [12]. Recently, diffusiophoresis has been widely used to design synthetic self-propelled microswimmers [17–26], where the swimmers catalyze chemical reactions to create local concentration gradients of solute molecules. The diffusiophoretic force arises from the interactions between particle and the surrounding inhomogeneous fluid environment induced by the solute concentration gradient  $\nabla c$ , and is proportional to  $\nabla c$  [12, 14, 15],

$$\mathbf{f} = \frac{\gamma D_{\text{DP}}}{c} \nabla c. \quad (1)$$

Here,  $\gamma$  and  $D_{\text{DP}}$  refer to the frictional coefficient and the diffusiophoretic mobility, respectively [14, 15]. For convenience, we define the coefficient  $\alpha_{\text{D}} \equiv \gamma D_{\text{DP}}/c$ , such that the diffusiophoretic force can be simply expressed as  $\mathbf{f} = \alpha_{\text{D}} \nabla c$ .

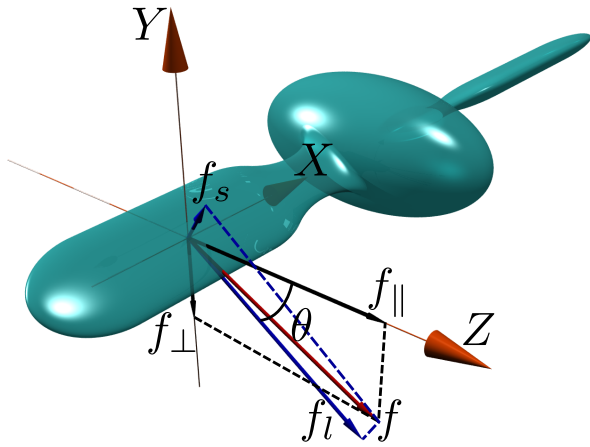


Figure 1: Sketch of a diffusiophoretic micro-turbine and the diffusiophoretic forces experienced by its blades. All the forces are in the  $y-z$  plane, with concentration gradient along the  $z$  axis.  $\mathbf{f}_l$  is parallel to the blade plane,  $\mathbf{f}_s$  perpendicular to it,  $\mathbf{f}_\parallel$  goes along  $z$  and  $\mathbf{f}_\perp$  on the  $y$  axis. The rotational direction of the turbine is parallel to the concentration gradient.

Equation (1) implies that the diffusiophoretic force always occurs in the direction of  $\nabla c$ , which is the case for isotropic particles characterized by a unique  $\alpha_D$ . This picture is however not generally valid for anisotropic particles, whose diffusiophoretic description is expected to need multiple  $\alpha_D$  (tensor). In the presence of an external temperature gradient, we have recently shown that an anisotropic object requires multiple thermodiffusion factors to correctly describe its thermophoretic behavior [27] and, as a consequence, the temperature gradient may then exert a torque on it. The similarity between thermophoresis and diffusiophoresis thus suggests that we could obtain a torque from an external concentration gradient by using anisotropic particles.

To analyze the feasibility, we here consider a propeller-like microscale object in a solution with concentration gradient along  $z$  axis, as shown in Fig. 1. This device consists of two connected blades with opposite orientation with respect to  $z$ . Here, the orientation angle of a blade ( $\theta$  in Fig. 1) is defined as the angle between the blade plane and the concentration gradient direction. Without loss of generality, we confine the left-blade orientation angle,  $\theta$ , in the range of  $[-\pi/2, 0]$ , and by constructing the right-blade orientation angle,  $\theta'$ , as opposite to the left one,  $\theta' = -\theta$ . The diffusiophoretic anisotropy of each blade is characterized by different diffusiophoretic coefficients in the directions perpendicular and parallel to the blade plane,  $\alpha_{D,s}$  and  $\alpha_{D,l}$ . The difference between  $\alpha_{D,s}$  and  $\alpha_{D,l}$  mainly depend on the geometry and material properties of the blade. We first calculate the diffusiophoretic force on one blade (say the left one). The concentration gradient can be decomposed into the directions perpendicular and parallel to the blade plane,  $\sin\theta|\nabla c|$  and  $\cos\theta|\nabla c|$ , so the diffusiophoretic forces in

these two directions are separately written as,

$$\mathbf{f}_s = \alpha_{D,s} \sin\theta |\nabla c| \mathbf{n}_s \quad (2)$$

and

$$\mathbf{f}_l = \alpha_{D,l} \cos\theta |\nabla c| \mathbf{n}_l \quad (3)$$

Here,  $\mathbf{n}_s$  and  $\mathbf{n}_l$  are the unit vectors perpendicular and parallel to the blade plane, respectively. The total diffusiophoretic force on the blade is then  $\mathbf{f} = \mathbf{f}_s + \mathbf{f}_l$ .

A remarkable feature of the anisotropic diffusiophoresis is that the diffusiophoretic force generally has a non-vanishing component perpendicular to the concentration gradient,  $\mathbf{f}_\perp$ . With Eqs. (2) and (3), the diffusiophoretic forces along and normal to  $\nabla c$  read

$$\mathbf{f}_\parallel = (\alpha_{D,s} \sin^2\theta + \alpha_{D,l} \cos^2\theta) \nabla c, \quad (4)$$

and

$$\mathbf{f}_\perp = (\alpha_{D,l} - \alpha_{D,s}) \sin\theta \cos\theta |\nabla c| \mathbf{n}_\perp, \quad (5)$$

with  $\mathbf{n}_\perp$  being the unit vector perpendicular to  $\nabla c$ . For isotropic particles ( $\alpha_{D,s} = \alpha_{D,l}$ ),  $\mathbf{f}_\perp$  vanishes and Eq. (4) reduces to Eq. (1).

Due to the employed symmetry, the diffusiophoretic forces on the right blade have  $\mathbf{f}'_\parallel = \mathbf{f}_\parallel$  and  $\mathbf{f}'_\perp = -\mathbf{f}_\perp$ . Consequently, besides the diffusiophoretic force in the concentration gradient,  $2\mathbf{f}_\parallel$ , there exists a torque acting on the propeller-like object along  $\nabla c$ ,

$$\mathcal{T} = \mathbf{d} \times \mathbf{f}_\perp = d(\alpha_{D,s} - \alpha_{D,l}) \sin\theta \cos\theta \nabla c. \quad (6)$$

Here,  $\mathbf{d}$  is the separation between the centers of the two blades, with  $d = |\mathbf{d}|$ , and the forces on each blade are assumed to act on the blade centers. The torque is determined by  $\alpha_{D,s} - \alpha_{D,l}$ , the external concentration gradient,  $\nabla c$ , and the blade orientation  $\theta$ .

This diffusiophoretic torque can thus drive the microscale propeller to rotate unidirectionally around  $\nabla c$ . The rotation is generated from the diffusive mass flux in a constant concentration gradient, which resembles very much what a conventional turbine does in a convective flow, such as a water turbine. Hence, we name the present microrotor as *diffusiophoretic turbine*. When the driving torque is balanced by the hydrodynamic friction, the turbine reaches a steady rotational velocity,  $\omega = \mu_r \mathcal{T}$ , with  $\mu_r$  being the rotational mobility of the turbine. To obtain an analytical estimation of  $\mu_r$ , we approximate the whole turbine as a non-slip cylinder of length  $l_H$  and diameter  $d_H$ , which correspond to the turbine dimensions in  $x-y$  and  $z$  directions, respectively. In the Stokes regime, the rotational mobility is calculated  $\mu_r = 3\lambda/\pi\eta l_H^3$  [28], with  $\lambda = -\ln(d_H/l_H) - 0.662 + 0.917(d_H/l_H) - 0.05(d_H/l_H)^2$ . Considering Eq. (6) the steady angular velocity reads

$$\omega = \frac{3\lambda d \sin\theta \cos\theta (\alpha_{D,s} - \alpha_{D,l}) \nabla c}{\pi\eta l_H^3}. \quad (7)$$

Note that the proposed diffusiophoretic micro-turbine is significantly different from existing catalytic self-propelled rotors [29–36] in driving mechanisms and potential applications. The present turbine is passively driven by an external concentration gradient, which exists independently of the turbine. However, the catalytic self-propelled rotors are actively driven by a local concentration gradient which is produced by the rotor-catalyzed chemical reactions. Therefore, the diffusiophoretic turbine can harvest mechanical work from existing concentration gradients in environment; while the catalytic self-propelled rotors can not.

We emphasize that in the frame of phoresis, the present diffusiophoretic turbine and the previous thermophoretic turbine [27] share similar designing principle, but they have completely different potential applications. In particular, the anisotropic diffusiphoresis provides us a novel chemo-mechanical response, which could be applied to biological, biomimetic and chemical systems.

### SIMULATION METHOD

We perform computer simulations to examine the validity of the proposed scheme. We employ hybrid dynamic simulations to bridge the gap between the mesoscopic length and time scales of the micro-turbine and the atomic scales of the solution. The solution is modeled by a particle-based mesoscopic approach known as multiparticle collision dynamics (MPC) [37–41], while the micro-turbine is described by standard molecular dynamics (MD) method. In MPC, the solution is coarse-grained into a large number of point-like particles with simple collision rule, by which mass, linear momentum, angular momentum and energy can be locally conserved. The MPC algorithm has been proven to properly capture hydrodynamic behaviors, thermal fluctuations, mass transport and heat conduction, and has been widely used in studies of complex fluids and synthetic micromotors [19, 26, 38–44]. In the simulations we employ standard MPC parameters, and all quantities are dimensionless in terms of the MPC units. The dynamic viscosity of the solvent is around  $\eta \simeq 3.2$ . The simulation box is a cuboid of dimensions  $L_x = L_y = 50$  and  $L_z = 34$ , with periodic boundary conditions in the  $x$  and  $y$  directions and non-slip wall boundary [45] in the  $z$  direction.

In order to simulate a diffusiophoretic effect with an external concentration gradient, we consider a solution with equimolar species A and B. These two species couple to each other via MPC collisions [19, 26] and are only distinguishable in their collisions to the wall and to the turbine. To obtain a steady-state concentration gradient we perform complementary operations at both walls, on the wall at  $z = 0$ :  $A+W1 \rightarrow B+W1$ , while on the wall at  $z = L_z$ :  $B+W2 \rightarrow A+W2$  both with the same reaction probability  $\zeta$ . This is equivalent to a system connected to

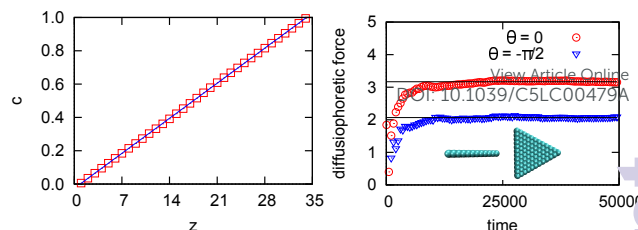


Figure 2: (a) Concentration distribution of  $B$ -solution particles in the steady state with  $\zeta = 1$ . (b) Diffusiophoretic forces acting on a fixed triangle blade as a time average, with the concentration gradient  $\nabla c = 0.03$ . The left and right insets correspond to the configurations of  $\theta = 0$  and  $\theta = -\pi/2$ , respectively.

two reservoirs with different concentrations. This boundary concentration-gradient-generator ensures that mass diffusion is correctly accounted for within the system. The magnitude of the gradient is tunable by changing reaction probability. Figure 2a displays a steady-state concentration gradient.

The turbine is composed of two connected triangular blades, as depicted in Fig. 3a. Each blade consists of a single layer of monomer beads of radii  $R = 1.25$ , mounted in the shape of a rigid equilateral triangle with edge length  $l = 11$ . A and B solution particles interact with the turbine beads via different repulsive Lennard-Jones potentials,  $U(r) = 4 \left[ \left( \frac{R}{r} \right)^{2n} - \left( \frac{R}{r} \right)^n \right] + 1$  for  $r \leq \sqrt[3]{2}l$ . Here,  $n = 3$  and  $n = 24$  are separately chosen for species A and B. This difference in the interaction potential leads to a measurable diffusiophoretic effect, which intuitively results from the mismatch between the forces exerted on the blade by species A and B due to inhomogeneous concentrations. In the simulations, the turbine center is fixed in the middle of the simulation box to avoid the drift of the entire turbine, and the turbine is allowed to rotate only around the  $z$ -axis, with the moment of inertia  $I = 2 \times 10^5$ . The equations of motion are integrated with a velocity-Verlet algorithm.

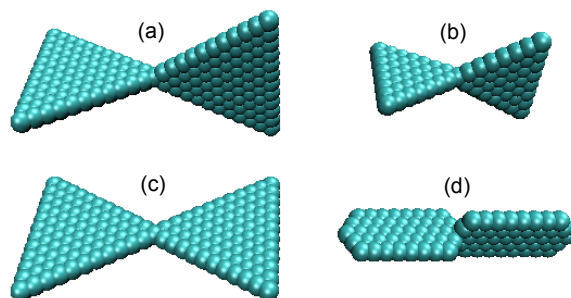


Figure 3: Simulation model of the diffusiophoretic micro-turbines. The turbines (a) and (b) have triangle blades but different sizes, with orientation angles  $\theta = -\theta' = -\pi/4$ . (c) Symmetric micro-turbine with  $\theta = \theta' = -\pi/4$ . (d) The blades of the turbine are hexagonal, with  $\theta = -\theta' = -\pi/4$ .



## RESULTS AND DISCUSSIONS

Before studying the motion of the turbine, we first test if the triangular blades of the turbine do show the anisotropic diffusiophoretic effect, by quantifying  $\alpha_{D,s}$  and  $\alpha_{D,l}$  in simulation. We consider a single blade fixed in space with its plane parallel ( $\theta = 0$ ) or perpendicular ( $\theta = -\pi/2$ ) to the concentration gradient, and measure the diffusiophoretic forces on it (see Fig. 2b). For these two configurations only the parallel component of the diffusiophoretic force,  $\mathbf{f}_{\parallel}$ , is nonzero. From Eq. (4) the ratios between the measured forces and  $\nabla c$  correspond to  $\alpha_{D,l}$  and  $\alpha_{D,s}$ , respectively. We thus obtain the coefficients  $\alpha_{D,l} \simeq 106$  and  $\alpha_{D,s} \simeq 71$ . So, the triangle blade is indeed diffusiophoretically anisotropic, which satisfies the necessary condition for the constructed diffusiophoretic turbine. Note that the precise values of  $\alpha_D$  are determined by the blade geometry and the solvent-turbine interaction potentials, but the relative diffusiophoretic anisotropy originating from the non-symmetric geometry of the blade is only weakly dependent on the specific choice of the potentials.

We then measure the rotational angle of the turbine,  $\varphi$ , averaged over realizations as a function of time, as plotted in Fig. 4. Results indicate that the externally applied concentration gradient induces a unidirectional rotation of the turbine, while simultaneously subject to thermal fluctuations, as shown in the inset of Fig. 4. For reference, we plot the result in the absence of diffusive mass flux, where the mean rotational angle of the turbine vanishes. Furthermore, for a symmetric turbine whose two blades are parallel to each other, i.e.  $\theta' = \theta$  (Fig. 3c), the torques exerted by the two blades cancel exactly such that the net rotation of the turbine vanishes. In addition, we also investigate the effect of the blade size and shape on the turbine rotation. We find that the use of smaller triangle blades (Fig. 3b) or hexagonal blades (Fig. 3d) only slightly change the rotational velocity in the present parameter regime.

In Fig. 5, we plot the angular velocity of the turbine depicted in Fig. 3a, as a function of the concentration gradient  $\nabla c$  and of the orientation angle of the blade  $\theta$ . The linear dependence of  $\omega$  on  $\nabla c$  and non-monotonic variation with  $\theta$  are consistent with the theoretical prediction in Eq. (7). For our simulation system, the Reynolds number can be determined as  $Re = \omega l^2 / \nu$ , with  $\nu = 0.32$  being the kinetic viscosity of the solvent. Under the maximum angular velocity, we obtain  $Re \sim 0.03$ , which is small enough to consider the validity of the Stokes limit employed in the derivation of Eq.(7). To quantitatively compare the simulation with the theoretical prediction, we need to quantify the distance between the centers of the blades  $d$ , and the length and diameter of the cylinder used to approximate the rotational mobility,  $l_H$  and  $d_H$ . Considering the structure of the turbine in Fig. 3a

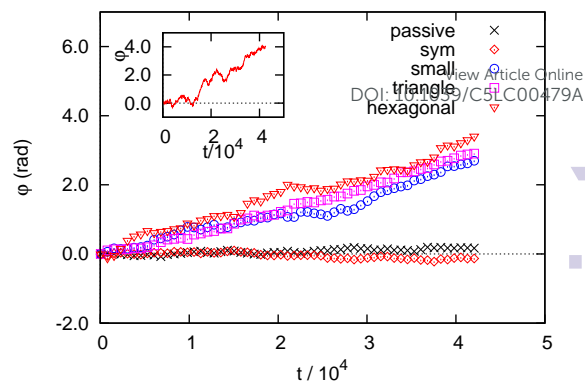


Figure 4: Averaged rotational angle as a function of time for different turbines, with the concentration gradient  $\nabla c = 0.03$ . Positive  $\varphi$  corresponds to the counterclockwise rotation of the turbines in Fig. 3. The notations triangle, small, sym and hexagonal separately refer to the turbines (a), (b), (c) and (d) in Fig. 3, and passive to the case of  $\nabla c = 0$ . Inset corresponds to an instantaneous trajectory of turbine (a).

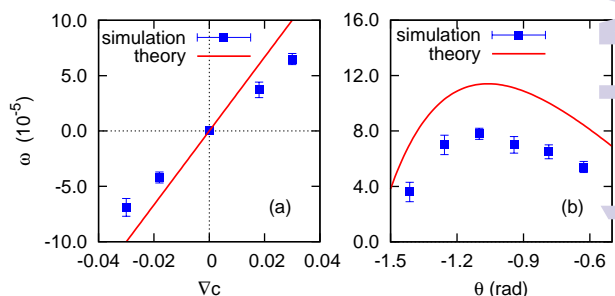


Figure 5: Angular velocity of the micro-turbine in Fig. 3a as a function of (a) the concentration gradient and (b) the orientation angle  $\theta$ , with the simulation units. Symbols correspond to the simulation results, and lines to the theoretical predictions from Eq. (7). In the case of (a),  $\theta = -\theta' = -\pi/4$ ; in the case of (b), the concentration gradient is set as  $\nabla c = 0.03$ .

and the size of the beads on the blade edges, we have  $d = 2\sqrt{3}l/3$ ,  $l_H = 2R + \sqrt{3}l$  and  $d_H = 2R + l \cos \theta$ . With these quantities and the previous measured  $\alpha_{D,l}$  and  $\alpha_{D,s}$ , the rotational velocity of the micro-turbine can be analytically determined from Eq. (7) without any adjustable parameter, as plotted in Fig. 5. This analytical calculation can very well describe the simulation results, except for a moderate overestimation for the magnitude of  $\omega$ . The deviation comes from the approximation used in the estimation of the rotational mobility and the implicit assumption in the analytical derivation that the local concentration distribution of the solute molecule near the turbine does not depend on the configuration of the turbine blade and its motion. Clearly, the latter assumption can be better satisfied for larger diffusivity of the solute.

In our simulations, the turbine dimensions are about 1/3 and 1/4 of the system box sizes in the x (y) and z directions, respectively. This corresponds to a weakly confined system, that is relevant in microfluidics. Thus,

finite size effects may play a role in the performance of the turbine. Given a constant external concentration gradient, finite size effects mainly arise from the influence of the system boundaries on the rotational flow field around the turbine. Since the present turbine is external torque-free, the resulted rotational velocity field is short-ranged, decaying as (at least)  $1/r^3$  faster than that of a passive turbine ( $1/r^2$ ). Therefore, the hydrodynamic finite size effects are weak and larger simulation boxes are expected to only slightly change the present quantitative results.

On the other hand, when the boundary walls come very close to the rotating turbine, interactions between the solvent flow and the walls will enhance the rotational rate of the turbine, since the walls exert a hydrodynamic frictional torque on the solvent in the direction of the turbine rotation (Note that the fluid and turbine have opposite rotational directions due to angular momentum conservation). Moreover, the boundary wall could also respond to the existing concentration gradient and induce an osmotic flow parallel to the walls. This diffusio-osmotic flow may further influence the turbine rotation.

We here comment on the experimental feasibility of the diffusiphoretic micro-turbine. The performance of such a micro-turbine depends on the diffusiphoretic coefficient  $\alpha_D$  and the concentration gradient. A recent experiment shows that a polystyren-carboxylate particle of diameter  $0.2\mu\text{m}$  in a solution of LiCl of concentration  $0.05M$  has a diffusiphoretic mobility  $D_{DP} \sim 300\mu\text{m}^2/\text{s}$  [14]. With the particle frictional coefficient obtained from Stokes law and the definition of the diffusiphoretic coefficient, we have  $\alpha_D \sim 1.2 \times 10^{-5} \text{kg}\mu\text{m}^2/\text{s}^2M$ . Thus, under a moderate concentration gradient  $\nabla c \sim 5 \times 10^{-4} M/\mu\text{m}$ , we roughly estimate from Eq. (7) that such a micro-turbine of  $\sim 0.2\mu\text{m}$  can rotate at  $\sim 5$  revolutions per second. The rotational velocity could be further enhanced by optimizing the geometry and the material of the turbine and by using large concentration gradients that are common in microfluidics due to extreme confinements. Therefore, this effect would be strong enough for practical applications. Additionally, since the diffusiphoresis can occur in both ionic and nonionic solutions [12], the proposed turbine can work in both types of solution environment.

Finally, we briefly discuss possible applications of this new device, particularly in the field of microfluidics. The diffusiphoretic turbine directly converts chemical energy in chemical gradients to mechanical work. It can be used as a micro-motor to power other microfluidic devices, which is a synthetic counterpart of biological rotors driven by diffusive ionic flux, e.g, the rotary motor of bacterial flagella [46]. Another obvious application of this turbine is as a stirring device (microfluidic mixer) to mix multiple components in microchannels. On the other hand, when the diffusiphoretic turbine is fixed by external constraints, the non-vanishing diffusiphoretic torque can produce a quasi-long-range ro-

tational flow field around the turbine, which constitutes a chemical gradient-driven rotational microfluidic pump. Furthermore, the diffusiphoretic turbine is an intrinsic chemo-mechanical sensor, which converts local chemical gradient into mechanical signal. The signal can then be employed to trigger valves or injection devices to actively control chemical gradients in microfluidic environments [47]. After calibration, such a sensor can be incorporated in microfluidic systems as an on-chip "chemical-gradiometer" that can measure local concentration gradient in-situ. This gradiometer is based on purely physical effect, such that is especially suitable for measuring concentration gradients of chemicals that participate in biochemical reactions. Lastly, anisotropic diffusiphoresis itself can induce a mechanical force, hence a motion, perpendicular to concentration gradient, which could be utilized to open or close channels, as chemical gradient-driven valves.

## CONCLUSIONS

We have shown that an external curl-free diffusive mass flow can generate a torque to rotate a microscale turbine. This scenario is reminiscent of the conventional turbines driven by convective particle flows, but with completely different physical essences. In the present case, the driving mechanism is based on anisotropic diffusiphoresis, which is an interesting but rarely studied effect. Moreover, the diffusiphoretic microturbine is also fundamentally distinguished from existing catalytic self-propelled microrotors [29–36], that actively "burn fuel" to generate motion, instead of passively extracting energy from surrounding environments. Our work therefore provides new insight into diffusiphoresis, and constitutes important, and until now missing, information on the chemo-mechanical response. In view of the potential applications of the novel chemo-mechanical effect, we hope that our work will stimulate experimental investigations.

## Acknowledgments

M.Y. gratefully acknowledges support from National Natural Science Foundation of China (Grant No. 11404379). This work was also supported by the MOST 973 Program (No. 2015CB856800). K.C. gratefully acknowledges the support from National Science Foundation of China (Grant No. 11474327) and the "The Recruitment Program of Global Youth Experts" from the government of China.

---

\* Electronic address: mcyang@iphy.ac.cn

† Electronic address: kechen@iphy.ac.cn

- [1] S. R. de Groot and P. Mazur, *Nonequilibrium thermodynamics* (Dover, New York, 1984).
- [2] S. K. W. Dertinger, D. T. Chiu, N. L. Jeon, and G. M. Whitesides, *Anal. Chem.* **73**, 1240 (2001).
- [3] J. Diao, L. Young, S. Kim, E. A. Fogarty, S. M. Heilman, P. Zhou, M. L. Shuler, M. Wu, and M. P. DeLisa, *Lab Chip* **6**, 381 (2006).
- [4] K. Sun, Z. Wang, and X. Jiang, *Lab Chip* **8**, 1536 (2008).
- [5] J. Atencia, J. Morrow, and L. E. Locascio, *Lab Chip* **9**, 2707 (2009).
- [6] E. Berthier and D. J. Beebe, *Lab Chip* **14**, 3241 (2014).
- [7] D. Brogioli, *Phys. Rev. Lett.* **103**, 058501 (2009).
- [8] W. Guo, L. Cao, J. Xia, F. Nie, W. Ma, J. Xue, Y. Song, D. Zhu, Y. Wang, and L. Jiang, *Adv Funct Mater* **20**, 1339 (2010).
- [9] B. E. Logan and M. Elimelech, *Nature* **488**, 313 (2012).
- [10] Z. Jia, B. Wang, S. Song, and Y. Fan, *Renew Sust Energ Rev* **31**, 91 (2014).
- [11] A. Siria, P. Poncharal, A.-L. Bianco, R. Fulcrand, X. Blase, S. T. Purcell, and L. Bocquet, *Nature* **494**, 455 (2013).
- [12] J. L. Anderson, *Annu. Rev. Fluid Mech.* **21**, 61 (1989).
- [13] B. Abécassis, C. Cottin-Bizonne, C. Ybert, A. Ajdari, and L. Bocquet, *Nature Mater.* **7**, 785 (2008).
- [14] J. Palacci, B. Abécassis, C. Cottin-Bizonne, C. Ybert, and L. Bocquet, *Phys. Rev. Lett.* **104**, 138302 (2010).
- [15] D. Prieve and R. Roman, *J. Chem. Soc., Faraday Trans.* **83**, 1287 (1987).
- [16] J. Ebel, J. L. Anderson, and D. Prieve, *Langmuir* **4**, 396 (1988).
- [17] R. Golestanian, T. B. Liverpool, and A. Ajdari, *Phys. Rev. Lett.* **94**, 220801 (2005).
- [18] J. R. Howse, R. A. L. Jones, A. J. Ryan, T. Gough, R. Vafabakhsh, and R. Golestanian, *Phys. Rev. Lett.* **99**, 048102 (2007).
- [19] G. Rückner and R. Kapral, *Phys. Rev. Lett.* **98**, 150603 (2007).
- [20] Y. Hong, N. M. K. Blackman, N. D. Kopp, A. Sen, and D. Velegol, *Phys. Rev. Lett.* **99**, 178103 (2007).
- [21] J. Palacci, C. Cottin-Bizonne, C. Ybert, and L. Bocquet, *Phys. Rev. Lett.* **105**, 088304 (2010).
- [22] L. F. Valadares, Y. G. Tao, N. S. Zacharia, V. Kitaev, F. Galembeck, R. Kapral, and G. A. Ozin, *Small* **6**, 565 (2010).
- [23] B. Sabass and U. Seifert, *J. Chem. Phys.* **136**, 064508 (2012).
- [24] I. Buttinoni, J. Bialké, F. Kümmel, H. Löwen, C. Bechinger, and T. Speck, *Phys. Rev. Lett.* **110**, 238301 (2013). View Article Online  
DOI: 10.1039/C5SL00479A
- [25] J. Palacci, S. Sacanna, A. P. Steinberg, D. J. Pine, and P. M. Chaikin, *Science* **339**, 936 (2013).
- [26] M. Yang, A. Wysocki, and M. Ripoll, *Soft Matter* **10**, 6208 (2014).
- [27] M. Yang, R. Liu, M. Ripoll, and K. Chen, *Nanoscale* (2014).
- [28] M. M. Tirado, C. L. Martínez, and J. G. de la Torre, *J. Chem. Phys.* **81**, 2047 (1984).
- [29] J. M. Catchmark, S. Subramanian, and A. Sen, *Small* **1**, 202 (2005).
- [30] S. Fournier-Bidoz, A. C. Arsenault, I. Manners, and G. A. Ozin, *Chem. Commun.* pp. 441–443 (2005).
- [31] L. Qin, M. J. Banholzer, X. Xu, L. Huang, and C. A. Mirkin, *J. Am. Chem. Soc.* **129**, 14870 (2007).
- [32] Y. He, J. Wu, and Y. Zhao, *Nano Lett.* **7**, 1369 (2007).
- [33] Y. Wang, S. Fei, Y. Byun, P. E. Lammert, V. H. Crespi, A. Sen, and T. E. Mallouk, *J. Am. Chem. Soc.* **131**, 9923 (2009).
- [34] S. Ebbens, R. A. L. Jones, A. J. Ryan, R. Golestanian, and J. R. Howse, *Phys. Rev. E* **82**, 015304(R) (2010).
- [35] J. Gibbs, S. Kothari, D. Saintillan, and Y. Zhao, *Nano Lett.* **11**, 2543 (2011).
- [36] M. Yang, M. Ripoll, and K. Chen, *J. Chem. Phys.* **142**, 054902 (2015).
- [37] A. Malevanets and R. Kapral, *J. Chem. Phys.* **110**, 8603 (1999).
- [38] J. T. Padding and A. A. Louis, *Phys. Rev. E* **93**, 031401 (2006).
- [39] R. Kapral, *Adv. Chem. Phys.* **140**, 89 (2008).
- [40] G. Gompper, T. Ihle, D. M. Kroll, and R. G. Winkler, *Adv. Polym. Sci.* **221**, 1 (2009).
- [41] M. Yang and M. Ripoll, *Soft Matter* **9**, 4661 (2013).
- [42] M. Yang and M. Ripoll, *Phys. Rev. E* **84**, 061401 (2011).
- [43] R. Kapral, *J. Chem. Phys.* **138**, 020901 (2013).
- [44] M. Yang and M. Ripoll, *Soft Matter* **10**, 1006 (2014).
- [45] A. Lamura, G. Gompper, T. Ihle, and D. M. Kroll, *Biophys. Lett.* **56**, 319 (2001).
- [46] H. C. Berg, *Annu. Rev. Biochem.* **72**, 19 (2003).
- [47] B. G. Chung, F. Lin, and N. L. Jeon, *Lab Chip* **6**, 714 (2006).